Theoretical Calculations on $C_{30}H_{12}$ Bowl-Shaped Hydrocarbons: NMR Shielding Constants, Stability, and Aromaticity

SANTIAGO MELCHOR FERRER, JOSE MOLINA MOLINA

Grupo de Modelización y Diseño Molecular, Instituto de Biotecnología, Campus Fuentenueva, Universidad de Granada, E-18071 Granada, Spain

Received 29 March 1999; accepted 3 May 1999

ABSTRACT: Density Functional Theory (DFT) calculations at the B3LYP/6-31G* level have been performed on four bowl-shaped polyaromatic hydrocarbons of $C_{30}H_{12}$ molecular formula (**1**–**4**) showing C_3 (**1**), C_{2v} (**2** and **4**), and C_{2h} (**3**) symmetries. The geometrical and electronic properties of the compounds studied have been analyzed to explain their relative stability. NMR chemical shifts parameters for the atoms and Nucleus Independent Chemical Shifts (NICSs) for the rings were calculated using the GIAO method. The ^{13}C and ^{1}H chemical shifts calculated are in very good agreement with the experimental data. © 1999 John Wiley & Sons, Inc. J Comput Chem 20: 1412–1421, 1999

Keywords: fullerene; *ab initio* calculations; NMR; aromaticity; DFT; NICS

Introduction

In recent years, considerable attention has been focused on the family of fullerenes[1] and carbon nanotubes,[2] due to their unusual properties and useful applications.[3] In fact, one of the most challenging characteristics of nanotubes is the capability of their being conducting or semiconducting depending on their geometry,[4,5] opening the way to a new field of electronics (nanoelectronics), given that the joining of a conducting and a semiconducting nanotube leads to diode behavior,[6–8] the size of which is approximately a few dozen nanometers. More complex junctions between tubes may also have useful properties for constructing different nanometer-scale components.[9,10]

Correspondence to: J. M. Molina; e-mail: jmolina@goliat.ugr.es

CCC 0192-8651 / 99 / 131412-10

Within this context, we have previously performed calculations of the electronic-packet transmission in two-nanotube junctions.[11] These junctions are constructed by the insertion of an heptagonal and a pentagonal ring into the nanotube.[12] Unfortunately, these configurations do not appear frequently in the normal synthesis of nanotubes,[13,14] and there is no possible experimental control of the characteristics of the heptagon–pentagon pair (relative position between pentagon and heptagon). This contrasts with recent developments of intelligent synthesis methods of Bucky-bowls,[15–18] where the experimental method forces the presence of pentagons into the desired position. Developments in this field would enable in the near future the construction of nanotube junctions at will.

Both the structural properties of nanotube junctions and Bucky-bowls are our main interests, as the exact knowledge of the geometry of these compound is the first step in the investigation of their properties. We also seek reliable computational tool able to investigate different Carbon clusters, mainly nanotubes. In this context, calculations on Carbon nanotubes using a tight-binding approximation have been previously performed by our group to calculate several nanotube properties.[19]

Recently, Bucky-bowls with 30 or more carbon atoms have been synthesized and characterized by NMR spectroscopy,[15–17] or X-ray crystallography,[20] giving sufficient data to compare with *ab initio* calculations. Calculations on similar or the same compounds appear in the literature.[15,16,21,22] In addition, Schulman and Disch[23] reported accurate calculations on structure **1**, including geometries, POAV1 angles, and chemical shift values.

Theoretical methods of substantial quality can be used to calculate NMR data using the GIAO method,[24] yielding data comparable with the experiment. Nucleus Independent Chemical Shifts (NICSs)[25] calculations have been defined and used in the aromaticity or antiaromaticity characterization of several structures.[26]

The aim of the present work is to test various basis sets and computational methods applied in the calculation of the Bucky-bowl structures, to determine whether the method used is appropriate or not, using the calculation of NMR data and its comparison with experimental results. In addition, the geometrical and electronic properties of the calculated structures are discussed. The molecules considered in the article are shown in Figure 1.

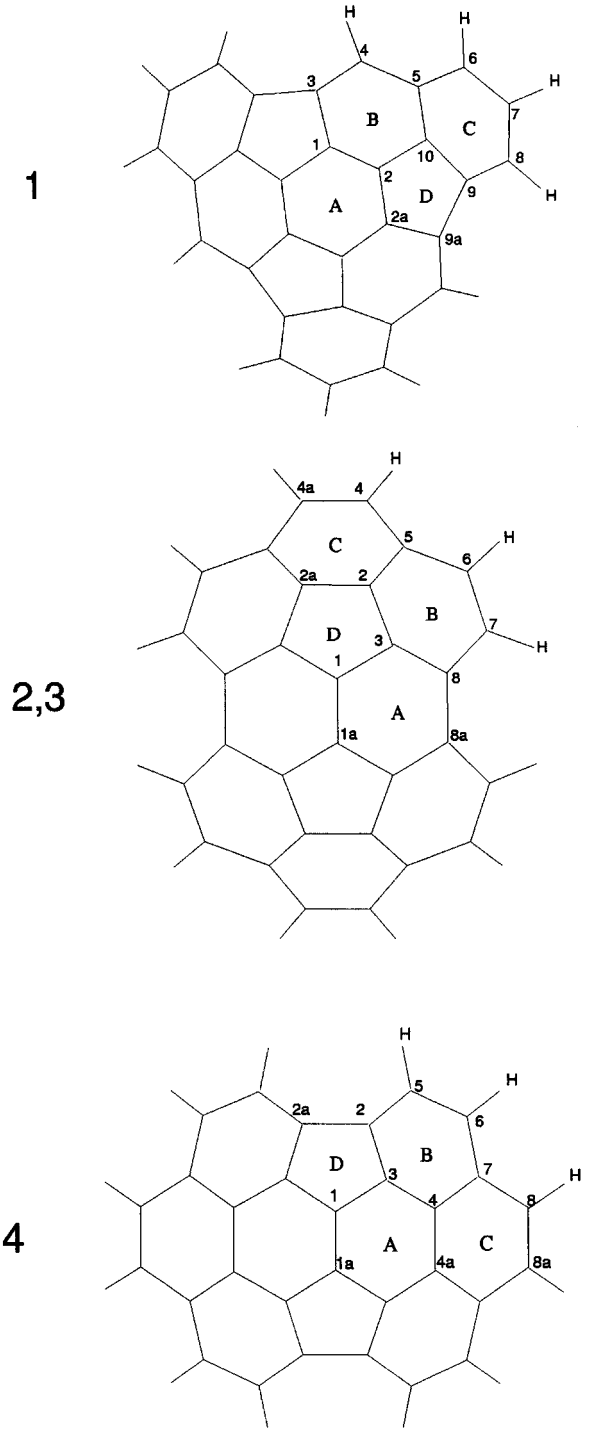

FIGURE 1. Labeling of the symmetry-independent atomic positions in structures **1**–**4**. Carbon positions are marked with integer numbers. Hydrogen independent positions are also shown. Numbers followed by ''a'' are used only in the bond description. Structures **2** and **3** use the same labeling because they have the same topology. Independent rings are marked by capitals A–D.

Theoretical Methods

The *ab initio* B3LYP[27] density-functional method (DFT) geometry optimizations were carried out using the Gaussian 94[28] and Gaussian 98[29] series of programs. The 6-31G* basis set was used for this purpose, and the respective symmetry restrictions for each molecule were explicitly imposed in the optimization. Calculations of the isotropic shielding in the Carbon and Hydrogen atoms and NICSs were performed using the GIAO method.[24] The chemical shift was obtained by subtracting the isotropic shielding of the carbon and hydrogen atoms from the corresponding shieldings in the TMS. The resulting geometries were discussed by means of the POAV1 analysis[30] and puckering parameters[31] for hexagonal and pentagonal rings, using the POAV3[32] and CONPUC[33] programs. In addition, a stress parameter has been defined (S) for each atomic position as the sum of the absolute differences between the interatomic angles at the carbon position and 120° (sp^2 configuration). Although the pyramidalization angles (POAV1 angles) and S parameters are defined for atoms, they can be used to characterize the rings and the entire structure by simply adding the absolute values (to avoid cancellations) in the respective carbon positions.

Results and Discussion

As was pointed out in the Introduction, calculations have been performed on structures **1**–**4** (see Fig. 1). Structures **1**, **2**, and **4** have previously been synthesized, and experimental data are available elsewhere.[15–17] Structure **3** is a conformational isomer of **2**, in which two opposite concavities are present. The numerical data obtained are summarized in Tables I–V. Table I presents the geometrical bond parameters and electronic properties of the bond critical points. Table II shows the overall data obtained for all the structures, as energies at different levels of theory, dipole moment, and geometrical parameters that measure curvature (POAV1) and stress (S) over entire structures. The overall ring properties as puckering parameters, NICS values, geometrical data, and the electronic ring properties of the critical points are presented in Table III, and the corresponding atomic data as well as ^{13}C-NMR Shielding constants, POAV1 angles, and S parameters are presented in Table IV. The ^{1}H-NMR spectra calculated are summarized in Table V. The numbering of the atoms and bonds and the ring denotation are included in Figure 1.

Figure 2 presents the theoretical three-dimensional geometries calculated for structures **1**–**4**. Structures **1**–**4** show different kinds of symmetry. **1** belongs to C_3, **2** and **4** to C_{2v}, and **3** to C_{2h} point groups. The above symmetries yield to a different number of independent atomic positions. The carbon positions are marked in Figure 1 with integer numbers and the hydrogen positions with an ''H.'' The numbers followed by an ''a'' are used to denote the bonds, but they are not independent positions. The symmetry independent rings are labeled by capital letters A–D.

Structures **1**–**4** are $C_{30}H_{12}$ hydrocarbons, and their theoretical geometries are depicted in Figure 2. Structures **1**, **2**, and **4** show only one concavity, while **3** shows two opposing ones. Structure **1** has three five-membered rings, and seven six-membered rings, while **2**, **3**, and **4**, have eight and two six and five-membered rings, respectively.

The bond distances are depicted in Table I, in which different ranges of bond lengths are obtained. These vary from 1.378 to 1.514 Å for **1**, 1.354 to 1.484 Å for **2**, 1.326 to 1.545 Å for **3**, and 1.354 to 1.522 Å for **4**. For **1**, the shortest bond distances correspond to bond C1—C2, but the C3—C4, C6—C7, and C8—C9 bonds also have a large double-bond character in the normal Kekulé structures. However, the greatest bond length is found in the C9—C9a bond, which has a clear single-bond character. This single bond belongs to a five-membered ring, not in common with any six-membered ring. For **2**, the shortest bond is the central C1—C1a bond, with a bond length of 1.354 Å, which is close to the normal C—C double-bond length. In this case, the longest bond is C8—C8a (1.484 Å), which is considerably shorter than a normal C—C single bond, given that the five pentagon bonds are common to the other hexagons. Compound **3**, however, shows the shortest (C1—C1a) and longest bond lengths (C8—C8a), totally compatible with double and single bonds, respectively, due to the tension produced by the two opposing concavities, in comparison with **2**. For **4**, the central C1—C1a bond also has a large double-bond character. However, C2—C2a bonds are almost single bonds, belonging to a pentagon and not being common to an hexagon.

The nature of the different bonds in compounds **1**–**4** has been analyzed from its electronic properties obtained at the corresponding bond critical

TABLE I.

1–4 C—C Bond Lengths (Å) and Electronic Properties Measured at the Bond Critical Point (Electronic Density ρ (ea_0^{-3}), Laplacian of the Electronic Density $\nabla^2\rho$ (ea_0^{-5}), Electronic Energy Density $E_d(r_c)$ (Hartrees a_0^{-3}), Ellipticity ε and Coefficient Between the Absolute Values of the Higher and the Lower Curvatures of the Hessian Matrix of ρ) Obtained at B3LYP/6-31G*//B3LYP/6-31G*.

Bond (Structure)	Distance	$\rho(r_c)$	$\nabla^2\rho(r_c)$	$E_d(r_c)$	ε	λ_1 / λ_3
1–2 (**1**)	1.378	0.330	−1.013	−0.355	0.243	2.64
1–3 (**1**)	1.443	0.300	−0.872	−0.295	0.154	2.08
3–4 (**1**)	1.392	0.319	−0.930	−0.334	0.324	2.52
4–5 (**1**)	1.457	0.286	−0.798	−0.270	0.159	1.99
5–10 (**1**)	1.414	0.313	−0.931	−0.320	0.203	2.31
5–6 (**1**)	1.423	0.306	−0.908	−0.307	0.180	2.23
6–7 (**1**)	1.391	0.321	−0.958	−0.338	0.293	2.57
7–8 (**1**)	1.422	0.305	−0.898	−0.306	0.192	2.25
8–9 (**1**)	1.385	0.325	−0.984	−0.346	0.280	2.60
9–9a (**1**)	1.514	0.257	−0.669	−0.223	0.084	1.68
9–10 (**1**)	1.424	0.304	−0.884	−0.302	0.176	2.15
10–2 (**1**)	1.406	0.321	−0.993	−0.335	0.150	2.37
2–2a (**1**)	1.428	0.306	−0.905	−0.306	0.139	2.16
1–1a(**2**)	1.354	0.348	−1.130	−0.395	0.258	3.04
1–3 (**2**)	1.431	0.305	−0.902	−0.304	0.135	2.15
2–3 (**2**)	1.424	0.308	−0.910	−0.310	0.157	2.19
2–2a (**2**)	1.432	0.303	−0.892	−0.302	0.144	2.15
4–4a (**2**)	1.382	0.325	−0.958	−0.346	0.352	2.67
4–5 (**2**)	1.447	0.293	−0.847	−0.282	0.137	2.06
5–2 (**2**)	1.390	0.328	−1.011	−0.350	0.230	2.55
5–6 (**2**)	1.439	0.297	−0.861	−0.289	0.153	2.10
6–7 (**2**)	1.388	0.321	−0.942	−0.338	0.332	2.59
7–8 (**2**)	1.443	0.296	−0.854	−0.287	0.160	2.09
8–3 (**2**)	1.407	0.315	−0.924	−0.324	0.250	2.36
8–8a (**2**)	1.484	0.272	−0.732	−0.245	0.137	1.83
1–1a (**3**)	1.326	0.367	−1.231	−0.440	0.306	3.68
1–3 (**3**)	1.415	0.315	−0.974	−0.325	0.101	2.27
2–3 (**3**)	1.412	0.313	−0.937	−0.322	0.162	2.28
2–2a (**3**)	1.446	0.298	−0.872	−0.292	0.136	2.09
4–4a (**3**)	1.388	0.321	−0.932	−0.339	0.370	2.61
4–5 (**3**)	1.461	0.285	−0.810	−0.269	0.120	1.97
5–2 (**3**)	1.385	0.331	−1.035	−0.357	0.223	2.59
5–6 (**3**)	1.442	0.294	−0.835	−0.284	0.178	2.09
6–7 (**3**)	1.410	0.308	−0.876	−0.312	0.307	2.35
7–8 (**3**)	1.438	0.296	−0.843	−0.289	0.198	2.11
8–3 (**3**)	1.399	0.320	−0.952	−0.335	0.252	2.43
8–8a (**3**)	1.545	0.241	−0.594	−0.198	0.072	1.57
1–1a (**4**)	1.354	0.347	−1.116	−0.393	0.259	3.03
1–3 (**4**)	1.418	0.314	−0.964	−0.322	0.119	2.26
2–3 (**4**)	1.416	0.315	−0.929	−0.323	0.215	2.29
3–4 (**4**)	1.408	0.314	−0.938	−0.322	0.201	2.35
2–2a (**4**)	1.522	0.252	−0.642	−0.215	0.087	1.65
2–5 (**4**)	1.404	0.314	−0.935	−0.324	0.233	2.39
5–6(**4**)	1.411	0.310	−0.906	−0.315	0.249	2.35
6–7 (**4**)	1.417	0.308	−0.899	−0.310	0.222	2.28
7–4 (**4**)	1.419	0.312	−0.931	−0.317	0.188	2.26
7–8 (**4**)	1.449	0.293	−0.859	−0.283	0.115	2.05
4–4a (**4**)	1.446	0.293	−0.842	−0.283	0.148	2.05
8–8a (**4**)	1.370	0.332	−0.998	−0.362	0.374	2.85

TABLE II.
Energies Calculated at HF and B3LYP Levels (Hartrees), Dipole Moment (Debyes), and Sums of POAV1 and S Parameters (Degrees) for Structures 1–4.

	1	2	3	4
HF/6-31G*//B3LYP/6-31G*	−1142.98054391	−1143.00913927	−1142.92884129	−1143.04127811
B3LYP/6-31G*//B3LYP/6-31G*	−1150.38125679	−1150.40379277	−1150.33056169	−1150.43598245
Dipole moment	3.43	3.40	0	2.85
Sum of POAV1 angles	158.7	157.2	141.9	127.5
Sum of S angles	373.1	350.8	496.2	339.6

point, using the AIM theory.[34] In general, the C—C bonds are covalent (large electron density ρ, large negative Laplacian of the electron density $\nabla^2\rho$, large and negative electronic-energy density E_d and large λ_1/λ_3 values; see Table I). The multiple bond character has been associated with different electronic properties, so that the bond order for hydrocarbons can be fitted with the electron density at the bond critical point.[35] Table I shows a direct correlation between the bond lengths and the electron density, displaying larger ρ values with shorter bond lengths. In general, there is also an increase in ellipticity values, showing the higher anisotropy of the shorter bonds. However, in compounds **1**–**4**, there is some discrepancy about the possible bond orders and values of the ellipticity; the shortest C—C bond for **1** is C1—C2, and C1—C1a for **2**–**4**. All of these are internal bonds, in which the electron density is the highest, but the ellipticity for other bonds in the periphery with smaller electron density and larger bond lengths show higher values (C3—C4, C6—C7, and C8—C9 in **1**, C4—C4a in **2** and **3**, and C8—C8a in **4**). The increase of the ellipticity for the bonds in the periphery is due to a decrease in the λ_2 (negative curvature of the Hessian matrix in the π orbital direction). This decreasing corresponds with a increasing electron density in that area in comparison with the inner bonds, showing that the electron current is predominantly concentrated in the outer part of the molecule.

Structures **1**–**4** are different configurations of $C_{30}H_{12}$; their energies are depicted in Table II. Taking into account that the four structures have the same number of atoms and single and double bonds, we can determine their relative stability from their total energies. The order of stability is: **4** > **2** > **1** > **3**.The high instability of **3** can be explained from the ring tension due to the two opposing concavities presented. However, the rationalization of the order of stabilities in compounds **4**, **2**, and **1** has to be performed by analysis of different types of parameters, calculated both for rings of the different structures and for global structural parameters.

Structures **1**, **2**, and **4** show a bowl shape, presenting different ring deformation from the benzene planar disposition. This deformation has been analyzed using different parameters derived from geometric, magnetic, and electronic properties. Table III shows these ring parameters for structures **1**–**4**. All the structures show four different symmetry independent rings, three hexagons, and one pentagon in their structures. Structure **1** has seven hexagonal and three pentagonal rings. However, **2**–**4** have eight and two, respectively. One point that should contribute to the relative stability is the aromatic character of the different rings shown by the NICS values calculated in the center ($NICS_c$) of the rings and at points displaced 0.5 Å inside ($NICS_i$) and outside ($NICS_o$) the bowl, as suggested by Schleyer et al.[26] to avoid the effects of the σ bonds. Aromatic rings have negative NICS values, and antiaromatic ones have positive. In general, the hexagonal rings show different degrees of aromatic character, as opposed to the pentagonal ones, being antiaromatic.

In **1** and **2**, the three hexagons show strong aromatic character, while in structure **4**, ring B has the strongest aromatic character of the different rings of all structures, and rings A and C have low NICS values (see Table III), especially at the outer points. In general, the $NICS_o$ values are the lowest ones for each ring. From the aromaticity of the different rings, the overall stability of compounds **1**, **2**, and **4** should be the opposite to those calculated. This discrepancy could be explained taking into account some other parameters. Puckering parameters have been also calculated for structures **1**–**4**. In general, the puckering amplitude of the different rings are usually small, except in ring A of compound **3**, which has a large deformation, with parameters close to a twist conformation (see Table III). Usually the puckering amplitude is

TABLE III.

Puckering Amplitude (Å), φ and θ (Degrees), NICS Calculated 0.5 Å inside, in the Ring Center and 0.5 Å outside of the Bowl, Sum of POAV1 Angles, and S Parameters over the Rings (Degrees), Mean Bond Length of the Rings ML (Å), and Squared Mean Quadratic Deviation SMQD (Å).

	1				2				3				4				
Ring	A	B	C	D	A	B	C	D	A	B	C	D	A	B	C	D	Benzene
Puckering amplitude	0.0159	0.0985	0.1416	0.0662	0.0256	0.1589	0.1517	0.0621	0.395	0.1155	0.1154	0.091	0.0174	0.1229	0.1436	0.0463	0
φ	157	66.4	49.2	285.4	240	221.9	60	180	210	169.3	240	288	60	166.6	60	0	—
θ	179.8	87.4	70.3	—	90	97	90	—	90	86.1	90	—	90	103.4	90	—	—
$NICS_i$	−16	−15.6	−15	−3.5	−13.1	−15	−12.7	2.5	−2.5	−15.3	−9.1	3.9	−6.6	−15.4	−5.1	6.6	13.3
$NICS_c$	−7.9	−9.7	−11.1	1.8	−6.1	−9.9	−7.8	7.1	−0.2	−10.9	−4.9	7.5	−1.1	−11.1	−1.6	9.6	11.5
$NICS_0$	−3.5	−6.7	−10.5	2.5	−2.8	−8	−6.4	5.4	−2.5	−9.4	−4.4	4.9	0.2	−9.9	−1.6	8.3	13.3
POAV1 sum	63.78	44.02	20.24		53.54	31.9	28.58		48.66	28.45	26.76		47.4	25.41	19.7		0
S sum	79.5	89.2	72.6		92.8	78.6	75.2		141.4	112.8	91.8		65.2	75.1	37.8		0
ML	1.403	1.415	1.412	1.445	1.419	1.415	1.415	1.429	1.417	1.415	1.421	1.42	1.409	1.413	1.426	1.438	1.397
SMQD	0.06	0.067	0.044	0.081	0.096	0.054	0.069	0.008	0.159	0.049	0.087	0.028	0.068	0.013	0.069	0.095	0

TABLE IV.

Calculated and Experimental ^{13}C-NMR Spectra, POAV1 Angles, and S Angles (Degrees).

	1					2					3				4				
	HF	B3LYP	Exp.[a]	POAV1	S	HF	B3LYP	Exp.[b]	POAV1	S	HF	B3LYP	POAV1	S	HF	B3LYP	Exp.[c]	POAV1	S
1	156.48	147.82	153.1	100.39	13	148.66	138.95	145.4	101.22	11.2	130.68	126.58	101.18	10.9	148.34	143.42	149.48	99.97	12.6
2	148.69	141.30	148.3	100.87	13.5	137.70	130.89	136.8	98.51	16	142.17	134.72	98.26	14.7	139.12	133.32	139.65	95.34	34.1
3	143.70	140.28	144.9	97.57	29.6	143.45	135.85	142.0	99.72	19.7	133.71	124.98	98.86	28.5	140.20	133.89	140.13	98.09	15.9
4	127.90	120.15	127.4	93.83	4.5	126.42	121.23	126.8	91.79	3.5	127.97	122.62	91.43	5.8	132.79	126.58	132.84	95.64	4.1
5	133.96	128.91	135.4	94.53	13.3	129.39	122.39	128.6	93.99	18.1	133.59	126.07	93.69	25.4	124.37	117.42	125.15	91.4	3.1
6	128.35	121.37	128.3	91.18	0.9	126.86	121.33	127.3	92.17	3.8	126.24	121.50	91.53	7.4	126.23	121.68	130.10	92.2	6.6
7	125.71	121.51	125.0	91.61	6.4	126.10	120.40	125.5	91.68	5.5	132.48	125.51	91.82	5.5	133.13	126.75	133.99	92.74	11.3
8	122.25	115.12	120.7	91.13	4.1	138.76	131.91	137.3	95.83	15.5	131.84	127.13	94.29	31.3	126.20	121.06	126.86	91.47	3.5
9	137.10	133.11	138.2	94.96	32.6														
10	140.78	132.67	138.6	96.83	15.3														

[a] Ref. 15.
[b] Ref. 16.
[c] Ref. 17.

TABLE V.
^{1}H-NMR Calculated and Experimental Spectra.

	1 HF	**1** B3LYP	Exp.[a]	**2** HF	**2** B3LYP	Exp.[b]	**3** HF	**3** B3LYP	**4** HF	**4** B3LYP	Exp.[c]
4	8.22	7.65	7.85	7.68	7.23	7.42	7.87	7.42			
5									7.99	7.17	7.47
6	7.97	7.41	7.62	7.83	7.38	7.55	7.98	7.57	7.74	7.03	7.40
7	7.62	7.32	7.39	8.25	7.81	7.91	8.51	8.00			
8	8.03	7.53	7.67						7.51	6.73	7.18

[a] Ref. 15.
[b] Ref. 16.
[c] Ref. 17.

around 0.1 Å. Ring A of **1**, **2**, and **4** are almost planar, but they have the highest deformation, taking into account the POAV1 analysis for each ring. This is due to the disposition of the A ring in each structure. In all cases, there is no hydrogen bonded to the rings and some neighboring pentagons invariably exist, yielding to a higher pyramidalization. The rings that have lower POAV1 values are the outer rings with bonded hydrogens. Therefore, in structure **1**, ring C, with three hydrogens, has very low POAV1 ring values, and ring B, with only one hydrogen, yields intermediate POAV1 ring parameter. Structures **2** and **4** have two hexagons with two hydrogens each. Rings B and C of **2** and B of **4** have small and similar POAV1 ring values; however, ring C of **4** is the only hexagon that does not have any neighboring pentagon and, thus, has the lowest POAV1 value.

In this context, ring C of **4** also has the smallest S value, showing the low strain present in this ring. These S values are very high for all three independent hexagons of **3**, showing that this parameter represents complementary data of the POAV1 analysis and indicating that is a good representation of the ring strain. For example, ring A of structures **1** and **2** are almost planar (small puckering amplitude), show also larger S values. In addition, ring A of structure **4** (also almost planar) gives medium S and POAV1 ring values, sometimes showing parallel behavior. However, in some cases, discrepancies exist between the two parameters. Ring B of structure **4** has a very low POAV1 ring parameter and a high S value in comparison with the other hexagons of **4**, but small in comparison with all the hexagons of the other structures. In general, structure **4** yields to the smallest S values. Two geometrical parameters related with the deformation of the hexagonal rings in comparison with benzene ring are the mean bond length and the bond dispersion. The higher the bond dispersion , the lower conjugation of the double bonds and lower should be the aromaticity. Ring B of structure **4** has the smallest bond dispersion (0.013 Å), yielding one of the rings with the highest aromatic character ($NICS_i$ of -15.4) and also very high $NICS_c$ and $NICS_o$ values). In general, low values for the bond dispersion are compatible with high aromaticity. Ring C of structure **1**, B of **2**, and B of **3** also have high aromaticity. From the discussion presented so far, one clear conclusion emerges: the instability of structure **3**. It has the most distorted rings, with higher puckering amplitude, higher S values and the highest bond dispersion, especially for ring A, giving very high ring strain. However, the order of stability of **1**, **2**, and **4** cannot easily be obtained from the above analysis, and taking into account the electronic properties of the ring critical points in the center of the hexagons are mainly consistent with those obtained for benzene [ca. 0.0198 e a_0^{-3} and 0.163 e a_0^{-5} for $\rho(r)$ and $\nabla^2\rho(r)$, respectively].

Taking into account the difficulty discussed above, we shall now consider the overall geometric parameters in comparison with the calculated energies. The overall parameters chosen are the addition of the POAV1 angles and the S parameter for all the carbons of the structure. In Table II these overall parameters are depicted together with the energies of structures **1**–**4**. In comparing the two parameters, we find agreement with the calculated order of stabilities of structures **1**, **2**, and **4**. However, when we consider structure **3**, the POAV1 parameter gives the smallest values, but the highest value of the S parameter, showing the importance of using both parameters.

One of our main original interests was to test theoretical models to be applied to medium-sized carbon clusters with pentagons, hexagons, and heptagons. For this, we have made calculations on structures **1**, **2**, and **4**, for which experimental data

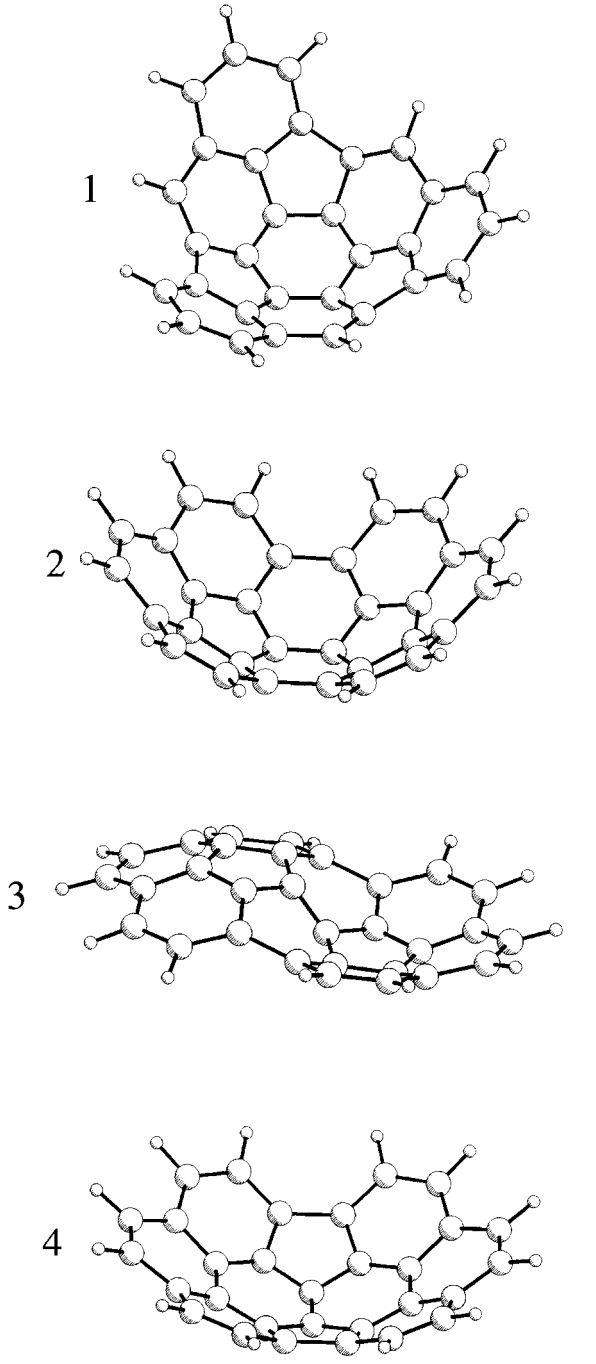

FIGURE 2. Three-dimensional plots of calculated structures **1**–**4**.

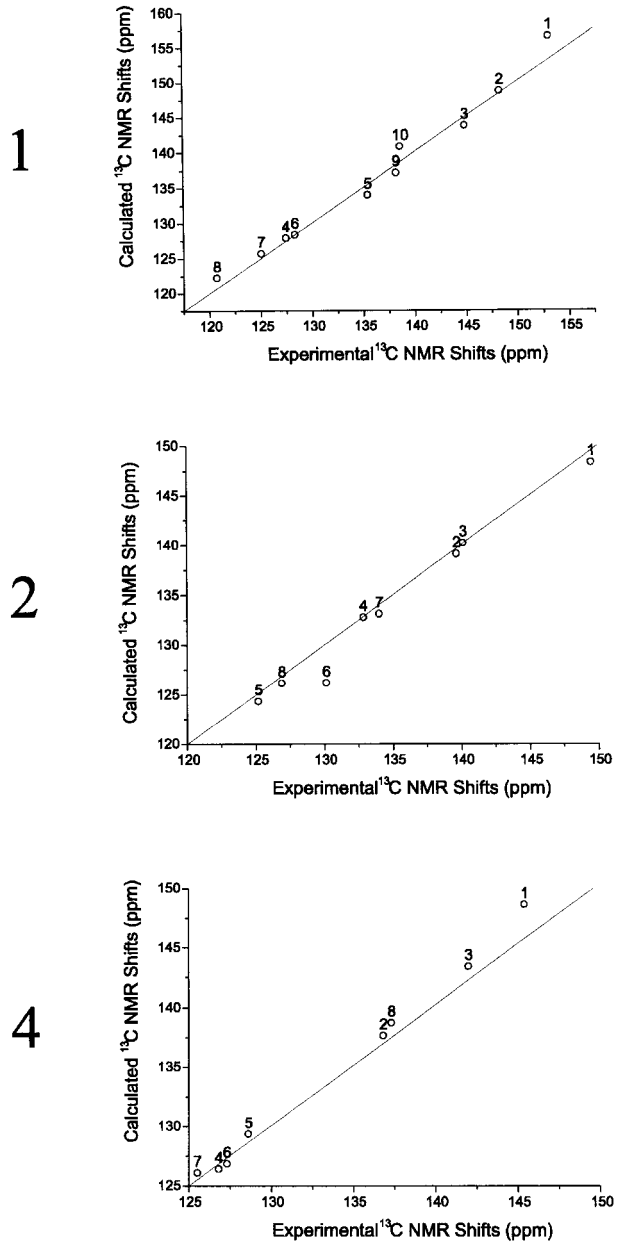

FIGURE 3. Plots of correlations between the predicted (HF/6-31G*//B3LYP/31G*) and measured ^{13}C chemical shifts for compounds **1**, **2**, and **4**.

are available. One property that can provide us orientation about the quality of the results is the NMR chemical shift shielding. So we have performed theoretical calculations of ^{13}C- and ^{1}H-NMR data to be compared with the experimental available data for **1**, **2**, and **4**. The results are presented in Tables IV and V, together with the experimental values when available, and plots of correlations between the predicted and measured chemical shifts are shown in Figure 3. The theoretical calculations have been performed at HF/6-31G* level from the theoretical geometries obtained at B3LYP/6-31G* level, as suggested elsewhere.[36] In Tables IV and V, the values obtained at the B3LYP/6-31G*//B3LYP/6-31G* theoretical level are also listed for comparison. The HF ^{13}C theoretical values are in very good agreement with the

experimental ones, for structures **1**, **2**, and **4**. However, our theoretical HF/6-31G*//B3LYP/6-31G* ^{13}C chemical shifts show a small disagreement with those reported by Schulman and Disch for **1** (mean deviation value = 1.56 ppm). The theoretical B3LYP values are systematically around 5 ppm lower. The ^{1}H-NMR data are shown in Table V, together with the experimental values. The overall agreement of the HF values with the experiment is good, including the assigned multiplicity; also, the B3LYP values are around 0.5 lower.

Conclusions

Accurate theoretical structures of different $C_{30}H_{12}$ polyaromatic hydrocarbons (**1**–**4**) have been obtained at the B3LYP/6-31G* level. Their geometrical parameters have been compared for the different configurations of **1**–**4** and with the electronic properties determined at the corresponding bond critical points.

Structure **3**, with two opposite concavities, shows great ring deformation and strain, giving rise to the least stable structure. The stabilities of **1**, **2**, and **4** have been discussed against different ring parameters; however, the calculated order of stability has been correlated with overall POAV1 and S geometrical parameters, revealing structure **4** as the most stable one, having the lowest values of POAV1 and S parameters.

The theoretical ^{13}C- and ^{1}H-NMR chemical shieldings calculated are in very good agreement with the experimental data, showing that the chosen theoretical level (B3LYP/6-31G*) is accurate enough to describe experimental data of medium-size carbon clusters.

Acknowledgments

We would like to thank Drs. A. Sygula and P. W. Rabideau for giving us the corrected experimental ^{13}C spectra of **2**, and Drs. R. C. Haddon and J. A. Pople for supplying the programs POAV 3.0 and CONPUC, respectively. We also thank David Nesbitt for the correction of the original manuscript.

References

1. Kroto, H. W.; Heath, J. R.; O'Brien, S. C.; Curl, R. F.; Smalley, R. Nature 1985, 318, 162.
2. Iijima, S. Nature 1991, 354, 56.
3. Dresselhaus, M. S.; Dresselhaus, G.; Eklund, P. C. Science of Fullerenes and Carbon Nanotubes; Academic Press: San Diego, 1995.
4. Hamada, N.; Sawada, S.; Oshiyama, A. Phys Rev Lett 1992, 68, 1579
5. Mintmire, J. W.; Robertson, D. H.; White, C. T. J Phys Chem Solids 1993, 54, 12, 1835.
6. Chico, L.; Benedict, L. X.; Louie, S. G.; Cohen, M. L. Phys Rev B 1996, 54, 2600.
7. Collins, P. G.; Zettl, A.; Bando, H.; Thess, A.; Smalley, R. E. Science 1997, 278, 100.
8. Saito, R.; Dresselhaus, G.; Dresselhaus, M. S. Phys Rev B 1996, 53, 2044.
9. Tans, S. J.; Verschueren, A. R. M.; Dekker, C. Nature 1998, 393, 49.
10. Menon, M.; Srivastava, D. Phys Rev Lett 1977, 79, 4453.
11. Melchor, S.; Khokhriakov, N. V.; Savinskii, S. S. Mol Eng, submitted.
12. Dunlap, B. I. Phys Rev B 1994, 49, 5643.
13. Lamb, L. D.; Huffman, D. R. J Phys Chem Solids 1993, 54, 1635.
14. Endo, M.; Takeuchi, K.; Igarashi, S.; Kobori, K.; Shiraishi, M.; Kroto, H. J Phys Chem Solids 1993, 54, 1841.
15. Abdouzarak, A. H.; Marcinow, Z.; Sygula, A.; Sygula, R.; Rabideau, P. W. J Am Chem Soc 1995, 117, 6410.
16. Rabideau, P. W.; Abdouzarak, A. H.; Folsom, H. E.; Marcinow, Z.; Sygula, A.; Sygula, R. J Am Chem Soc 1994, 116, 7891.
17. Hagen, S.; Brachter, M. S.; Erickson, M. S.; Zimmerman, G.; Scott, L. T. Angew Chem Int Ed Engl 1997, 36, 406.
18. Mehta, G.; Panda, G. Chem Commun 1997, 2081.
19. Khokhriakov, N. V.; Savinskii, S. S.; Molina J. M. JETP Lett 1995, 62, 617.
20. Shaltout, R. M.; Sygula, R.; Sygula, A.; Fronzek, F. R.; Stanley, G. G.; Rabideau, P. W. J Am Chem Soc 1998, 120, 835.
21. Sygula, A.; Rabideau, P. W. Chem Commun 1994, 1497.
22. Cioslowski, J.; Piskorz, P.; Moncrieff, D. J Org Chem 1998, 63, 4051.
23. Schulman, J. M.; Disch, R. L. J Comp Chem 1998, 19, 189.
24. Wolinski, K.; Hilton J. F.; Pulay, P. J Am Chem Soc 1990, 112, 821.
25. Schleyer, P. v R. J Am Chem Soc 1996, 118, 6317.
26. Zywietz, T. K.; Jiao, H.; Schleyer, P. v R.; Meijere, A. J Org Chem 1998, 63, 3417.
27. Becke, A. D. J Chem Phys 1993, 93, 5648.
28. Gaussian 94 Revision C.2, Frisch, M. J.; Trucks, G. W.; Schlegel, H. B.; Gill, P. M. W.; Johnson, B. G.; Robb, M. A.; Cheeseman, J. R.; Keith, T.; Petersson, G. A.; Montgomery, J. A.; Raghavachari, K.; Al-Laham, M. A.; Zakrzewski, V. G.; Ortiz, J. V.; Foresman, J. B.; Cioslowski, J.; Stefanov, B. B.; Nanayakkara, A.; Challacombe, M.; Peng, C. Y.; Ayala, P. Y.; Chen, W.; Wong, M. W.; Andres, J. L.; Replogle, E. S.; Gomperts, R.; Martin, R. L.; Fox, D. J.; Binkley, J. S.; Defrees, D. J.; Baker, J.; Stewart, J. P.; Head–Gordon, M.; Gonzalez, C.; Pople, J. A.; Gaussian, Inc.: Pittsburgh, PA, 1995.

29. Gaussian 98, Revision A.4, Frisch, M. J.; Trucks, G. W.; Schlegel , H. B.; Scuseria, G. E.; Robb, M. A.; Cheeseman, J. R.; Zakrzewski, V. G.; Montgomery, J. A.; Stratmann, R. E.; Burant, J. C.; Dapprich, S.; Millam, J. M.; Daniels, A. D.; Kudin, K. N.; Strain, M. C.; Farkas, O.; Tomasi, J.; Barone, V.; Cossi, M.; Cammi, R.; Mennucci, B.; Pomelli, C.; Adamo, C.; Clifford, S.; Ochterski, J.; Petersson, G. A.; Ayala, P. Y.; Cui, Q.; Morokuma, K.; Malick, D. K.; Rabuck, A. D.; Raghavachari, K.; Foresman, J. B.; Cioslowski, J.; Ortiz, J. V.; Stefanov, B. B.; Liu, G.; Liashenko, A.; Piskorz, P.; Komaromi, I.; Gomperts, R.; Martin, R. L.; Fox, D. J.; Keith, T.; Al-Laham, M. A.; Peng, C. Y.; Nanayakkara, A.; Gonzalez, C.; Challacombe, M.; Gill, P. M. W.; Johnson, B.; Chen, W.; Wong, M. W.; Andres, J. L.; Gonzalez, C.; Head−Gordon, M.; Replogle, E. S.; Pople, J. A.; Gaussian, Inc.: Pittsburgh, PA, 1998.
30. Haddon, R. C. Acc Chem Res 1998, 21, 243.
31. Cremer, D.; Pople, J. A. J Am Chem Soc 1975, 97, 1354.
32. Supplied by R. C. Haddon.
33. Evans, D. G.; Boeyens, J. C. A. Acta Crystallogr B 1989, 45, 581.
34. Bader, R. F. W. Atoms in Molecules; Oxford University Press: Oxford, 1990.
35. Bader, R. F. W. Atoms in Molecules; Oxford University Press: Oxford, 1990, p. 75.
36. Cheeseman, J. R.; Trucks, G. W.; Keith, T. A.; Frish, M. J. J Chem Phys 1996, 104, 5497.